A Surface-Potential-Based Compact Model of AlGaN/GaN HEMTs Power Transistors

P. Martin, R. Hahe and L. Lucci

CEA, Leti, Components Division, MINATEC Campus,
17 rue des Martyrs, 38054 Grenoble Cedex 9, France. patrick.martin@cea.fr

ABSTRACT

A physics based compact model for III-nitride HEMTs developed for SPICE circuit simulation of power transistors is presented. The HSP model (acronym for HEMT Surface-Potential model) follows a physical approach for power devices modeling, as it was done for advanced MOSFETs, leading to the development of compact models such as PSP, HiSIM and EKV3. This model includes: dependency on the aluminum content of energy bandgap and polarization, temperature dependency of several parameters and self-heating. Other effects, which are important when the HEMT transistor works at high voltage, high current and high temperature are also modeled.

Keywords: AlGaN/GaN HEMTs, MODFET, power transistor, compact model, surface potential

1 INTRODUCTION

High Electron Mobility Transistors (HEMT) based on the AlGaN/GaN heterojunction have already shown promising results for medium power (some Watts) microwave applications and industrialization of these components is already underway. There is now a challenging and very strong interest for high power transistors consisting in AlGaN/GaN HEMTs grown on cheap, large diameter substrates, in order to reduce costs, while achieving high performance energy conversion circuits, e.g. in automotive and aerospace applications. Several authors [1] have shown that 200 mm silicon substrates could be used for MOCVD growth of heterostructures, replacing much more expensive and smaller (less than 150 mm) silicon carbide substrates.

Given the complexity of technological processes (difficulty of donor implantation, refractory nature of wide band gap materials), there is also a need for developing compact SPICE models to simulate the electrical and thermal behavior of such transistors.

2 COMPACT MODELING OF HEMTS

A compact model is an optimal compromise between physical rigor and computation time and the choice of starting model is the first topic to be considered. We have indeed the choice between empirical and physical descriptions. Empirical models, such as Curtice [2] or Angelov [3] models, although not developed for HEMTs, are at present used for circuit simulation of power devices. However, there is a need for a more physical approach modeling, as it was done in the past ten years for bulk or SOI MOSFETs, leading to the development of PSP, HiSIM and EKV3 models and allowing precise simulation of very advanced CMOS technologies. A physical approach is preferred as it guarantees a better adaptability based on technological and physical parameters. A threshold voltage based model was developed by Rashmi [4] to describe physical phenomena of a HEMT transistor at different operating regimes. These regimes are then linked to each other by smoothing functions. However this treatment causes derivative discontinuities during the implementation in a simulator. The model presented by Cheng and Wang [5] is based on the calculation of surface potential in the channel. The notion of operating regimes no longer exists and the mathematical basis has already been demonstrated in the case of MOSFET. A surface-potential based model for GaN HEMTs for RF power amplifier applications was also developed [6] using the PSP model originally developed only for MOSFETs. A surface-potential based model was also described recently by Khandelwal [7].

In this paper we present a new physics based compact model called HSP (acronym for HEMT Surface-Potential model) as it is based on the analytical calculation of the Surface-Potential (SP) at the AlGaN/GaN interface. This model includes: dependency on the aluminum content of energy bandgap and polarization, temperature dependency of several parameters and self-heating. Other effects like series resistances, DIBL, velocity saturation and channel length modulation -which are important when the HEMT transistor works at high voltage, high current and high temperature- are also modeled.

3 HSP MODEL DESCRIPTION

Fig. 1 shows a cross-sectional view of an AlGaN/GaN HEMT. Table I gives the list of symbols used in this paper. The band structure of a vertical section under the Schottky gate is given in Fig. 2.

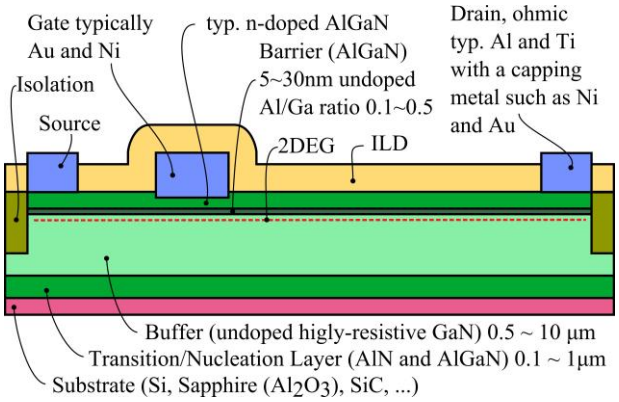

Fig. 1 Cross-sectional view of an AlGaN/GaN HEMT

Symbol	Definition	Units
n_s	Sheet electron density in 2-DEG	m^{-2}
$\varepsilon_{Al_xGa_{1-x}N}$	Dielectric constant of AlGaN	$C^2/J.m$
q	Elementary charge	C
k	Boltzmann's constant	J/K
T	Temperature	K
E_F	Fermi level	V
φ_B	Schottky gate barrier height	V
ΔE_C	Conduction band discontinuity	V
N_D	Donor concentration in n-AlGaN	m^{-3}
σ	Polarisation induced electron density	m^{-2}
d_d	Thickness of the n-doped AlGaN layer	m
d_i	Thickness of the undoped AlGaN layer	m
d	Total AlGaN thickness ($d_d + d_i$)	m
D_S	Conduction band density of states	m^{-2}/V
E_0	Lowest allowed energy level	V
u_1	Triangular well coefficient for E_0	$V.m^{4/3}$

Table 1: List of symbols

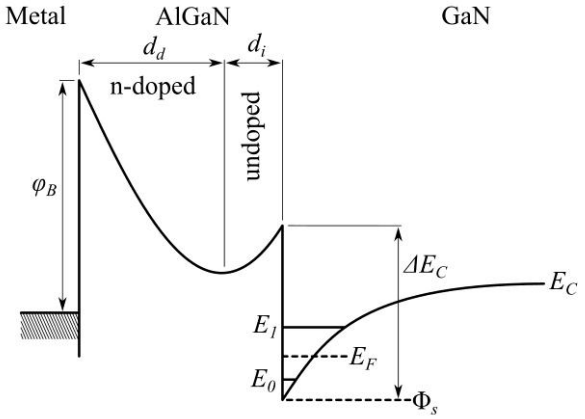

Fig. 2 AlGaN/GaN band structure

3.1 Electrostatics and 2-DEG charge density

This section describes electrostatics and quantum effects of the device and calculation of the 2-DEG sheet charge density. The equations of electrostatics are obtained by solving the Poisson equation in the approximation of fully ionized impurities. By solving the Schrödinger equation in 2D triangular approximation, the total system of equations becomes:

$$n_s = \frac{\varepsilon_{Al_xGa_{1-x}N}}{q\,d}\left(Vg - V_{off} - E_F\right) \quad (1)$$

$$V_{off} = \varphi_B - \Delta E_C - \frac{q\,N_D\,d_d^{\,2}}{2\,\varepsilon_{Al_xGa_{1-x}N}} - \frac{q\,\sigma}{\varepsilon_{Al_xGa_{1-x}N}}(d_d + d_i) \quad (2)$$

$$n_s = D\,kT\,Ln\left[1 + exp\left(\frac{E_F - E_0}{kT/q}\right)\right] \quad (3)$$

$$E_0 = u_1\,n_s^{\,2/3} \quad (4)$$

where Vg and V_{off} are gate voltage and offset voltage respectively. V_{off} could be either calculated from available literature [8, 9] or introduced as a parameter.

This system of equations is solved traditionally by a self-consistent numerical method. However, such a resolution is not suitable for a circuit simulator as it is too costly in computation time. Following the work of Cheng and Wang [5], this system could be solved analytically. Analytical determination of E_F ($E_F = \eta + \omega$) is done in two steps:

1 - Approximate solution (η) for two asymptotic cases: (a) for high n_s and (b) for low n_s,

2 - Small refinement (ω), important for medium n_s

Refinement is done several times (5-10) to ensure good accuracy for medium n_s. We obtain different analytical expressions than [5] and check that our expressions are valid even for very high Vds, up to 1 kV. The Fermi potential calculated for different thicknesses is shown in Fig. 3. A very good agreement with the numerical solution is obtained.

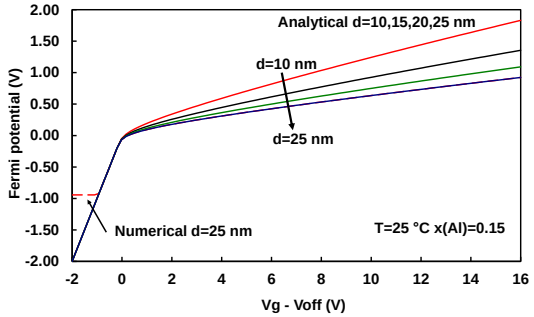

Fig. 3 E_F calculated for different total thicknesses d

Knowing the Fermi potential, the surface potential is given by:

$$\Phi_s = E_F + V_{ch} \quad (5)$$

Where V_{ch} is the channel voltage which varies between V_S at source and V_D at drain.

3.2 Mobility

The following mobility model is adopted [5]:

$$\mu_{LF}(E_T) = \frac{\mu_0}{1+\alpha|E_T|+\beta E_T^2} \quad (6)$$

where E_T is the transverse electrical field obtained from Gauss theorem at AlGaN/GaN interface:

$$\varepsilon_{GaN} E_T = \varepsilon_{AlGaN}(Vg - V_{off} - \Phi_{sm}) / d \quad (7)$$

Where Φ_{sm} = 0.5 (Φ_{sd} + Φ_{ss}) is known as the SP midpoint and where Φ_{ss} and Φ_{sd} are surface potentials calculated at source and drain, respectively.

3.3 Velocity saturation

The following velocity saturation model, where E_L is the longitudinal electrical field and E_c the critical field, is adopted [10]:

$$v_{drift}(E_L) = \mu_{LF}(E_T)\frac{|E_L|}{1+\left(\frac{|E_L|}{E_c}\right)} \quad (8)$$

3.4 DIBL Short channel effect

Drain-Induced Barrier Lowering (DIBL) effect is modeled as a shift of V_{off} with drain voltage Vds:

$$V_{off}(Vds) = V_{off}(0) - DIBL(Vd - Vs) \quad (9)$$

3.5 Temperature modeling

Some HSP model parameters, such as mobility μ_0, critical field E_c and thermal resistance R_{th}, are recalculated in temperature using the following law, where T_{ref} is a reference temperature and PEX an exponent:

$$P(T) = P(T_{ref})(T/T_{ref})^{PEX} \quad (10)$$

For V_{off}, temperature modeling is:

$$V_{off}(T) = V_{off}(T_{ref}) - TCV(T - T_{ref}) \quad (11)$$

3.6 Self-heating effect

Two models of the self-heating effect (SHE) are included:

1 – A simple model where an empirical thermal resistance R_{th} is assumed as a lumped element for the power dissipation P_{diss},

2 – A more physical approach that models the heat diffusion from channel through a substrate of thickness t_{sub} whose backside is held at constant temperature T_0 (heat sink). Assuming the following general law for thermal conductivity (KEX=-1.4 for GaN, -1.5 for SiC and -1.25 for GaAs):

$$\kappa(T) = \kappa(T_{ref})(T/T_{ref})^{KEX} \quad (12)$$

and following the approach of Canfield [11] to solve heat diffusion generated under the gate near the drain in a simple half-cylinder whatever the value of the KEX exponent, the temperature increase is given by:

$$\Delta T = T_0 \frac{1-\left(1-\frac{1}{\theta}\frac{P_{diss}}{P_0}\right)^{\theta}}{\left(1-\frac{1}{\theta}\frac{P_{diss}}{P_0}\right)^{\theta}} \quad (13)$$

$$with \quad \theta = -(KEX+1)^{-1}$$

$$and \quad P_0 = \pi\kappa(T_0) W T_0 \Big/ ln\left(\frac{8t_{sub}}{\pi L}\right) \quad (14)$$

Where W and L are gate width and length, α is a correction factor ($\alpha \leq 1$) allowing calculating the effective channel length from which heat dissipation occurs [12]. A new channel temperature is calculated (T' = T + ΔT) and all parameters depending on temperature are recalculated. Drain current is then updated. This process is repeated iteratively until convergence of drain current is attained. Less than 10 iterations are necessary for a less than 300 °C temperature increase.

3.7 Drain current model

Following the work of Gildenblat et al. [13] and using the concept of symmetric charge linearization introduced during development of the SP model, the drain current is calculated by:

$$I_{ds} = \beta \mu_{LF} \frac{(V_{gs} - V_{off} + V_t - \Phi_{sm})\Phi}{r_L + \delta_0 \Phi / V_c} \quad (15)$$

$$r_L = 1/(1 + \Delta L / L) \quad (16)$$

with β = W/L Cg, Cg = ε_{AlGaN} / d, Φ = Φ_{sd} – Φ_{ss}, r_L allows modeling of the channel-length modulation (CLM) effect and $V_c = E_c L$.

3.8 Charge model

The gate charge Qg, neglecting velocity saturation and CLM, is first calculated using the SP model formalism:

$$\frac{Q_g}{W\,L\,C_g} = q_{im} + \frac{\Phi^2}{12\,H}$$
$$q_{im} = V_g - V_{off} - \Phi_{sm}, H = q_{im} + \frac{kT}{q} \quad (17)$$

Source and drain charges are then evaluated using the Ward-Dutton partitioning scheme. If needed, intrinsic capacitances will be calculated as derivatives of the terminal charges: Cij = – dQi/dVj (i≠j) and Cii = dQi/dVi (i=j). Nine transcapacitances can be defined, six of them being independent. This treatment allows strict charge conservation during circuit simulation and requires no fitting parameters.

4 RESULTS

The model has been implemented using Verilog-A in the ADS simulator from Agilent. Results after parameter extraction on experimental data from literature [14] are presented in Fig. 4 and 5. Calculated intrinsic node charges are plotted in Fig. 6.

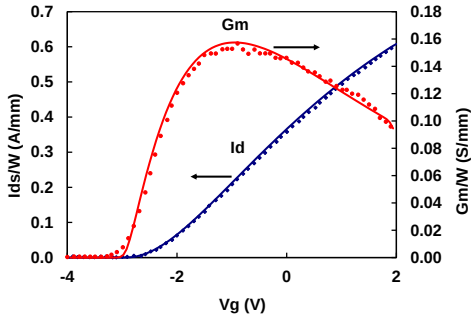

Fig. 4 Experimental (dots) and simulated (lines) Id(Vg) and Gm(Vg) characteristics (Vds=5 V, W=75 µm, L=1 µm)

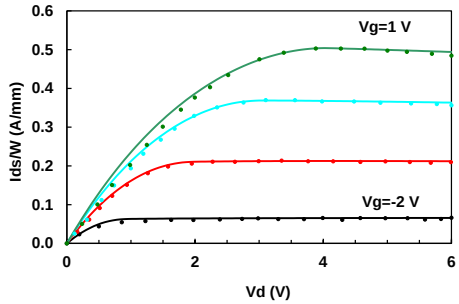

Fig. 5 Id(Vd) characteristics for Vgs=-2 V to 1 V step 1 V

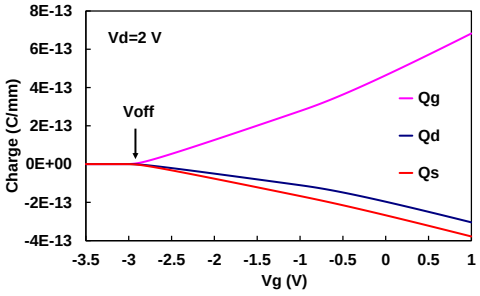

Fig. 6 Intrinsic node charges vs. gate voltage in saturation

5 CONCLUSION

We have developed an electro-thermal compact model using a surface-potential approach for power AlGaN/GaN HEMTs. We follow a physical approach enabling continuous calculation of drain current and charges with biases, temperature, AlGaN material properties, self-heating effects and heat diffusion in substrate. We hope this is an interesting tool for technological development and optimization of AlGaN/GaN HEMTs. Further research efforts are needed to improve the core model: e.g. improve the SHE algorithm for very high temperature increase (ΔT > 300 °C), modeling of surface traps effects and incomplete donor activation observed in refractory III-nitride compounds.

REFERENCES

[1] N. Vellas *et al.*, IEEE Electron Device Letters, vol. 23, n°8, pp. 461–463, 2002.

[2] W.R. Curtice and M. Ettenberg, IEEE Trans. on Microwave Theory and Techniques, vol. MTT–33, n°12, pp. 1383–1394, 1985.

[3] I. Angelov, V. Desmaris, K. Dynefors, P.Å. Nilsson, N. Rorsman and H. Zirath, 13th Gallium Arsenide and other semiconductor application symposium, Paris, pp. 309–312, 2005.

[4] Rashmi, A. Kranti, S. Haldar and R.S. Gupta, Solid-State Electronics 46, pp. 621–630, 2002.

[5] X. Cheng and Y. Wang, IEEE Trans. on Electron Devices, vol. 58, n°2, pp. 448–454, 2011.

[6] D.L. John *et al.*, IEEE Int. Electron Devices Meeting (IEDM), pp. 8.3.1–8.3.4, 2010.

[7] S. Khandelwal and T.A. Fjeldly, Solid-State Electronics, vol. 76, pp. 60–66, 2012.

[8] O. Ambacher *et al.*, J. of Applied Physics, vol. 85, n°6, pp. 3222–3233, 1999.

[9] T.-H. Yu and K.F. Brennan, IEEE Trans. on Electron Devices, vol. 50, pp. 315–323, 2003.

[10] C.C. Enz and E.A. Vittoz, "Charge-based MOS transistor modeling - The EKV model for low-power and RF IC design", John Wiley, 2006.

[11] P.C. Canfield, S.C.F. Lam and D.J. Allstot, IEEE J. Solid-State Circuits, vol. 25, n°1, pp. 299–306, 1990.

[12] A.-S. Royet, Contribution à l'optimisation d'une technologie de composants hyperfréquences réalisés en carbure de silicium (SiC), PhD thesis, INP Grenoble, 2000.

[13] G. Gildenblat, H. Wang, T.-L. Chen, X. Gu and X. Cai, IEEE J. Solid-State Circuits, vol. 39, n°9, pp. 1394–1406, 2004.

[14] Y.-F. Wu *et al.*, IEEE Electron Devices Letters, vol. 18, n°6, pp. 290–292, 1997.